Rate-of-change analysis in palaeoecology revisited: a new approach

Ondřej Mottl[1], John-Arvid Grytnes[1], Alistair W.R. Seddon[2], Manuel J. Steinbauer[1,3], Kuber P. Bhatta[1], Vivian A. Felde[2], Suzette G.A. Flantua[1], H. John B. Birks[2,4]

1. Department of Biological Sciences, University of Bergen, PO Box 7803, N-5020 Bergen, Norway
2. Department of Biological Sciences and Bjerknes Centre for Climate Research, University of Bergen, PO Box 7803, N-5020 Bergen, Norway
3. Bayreuth Center of Ecology and Environmental Research (BayCEER) and Department of Sport Science, University of Bayreuth, 95547 Bayreuth, Germany
4. Environmental Change Research Centre, University College London, Gower Street, London, WC1 6BT, UK.

Correspondence author:

Ondřej Mottl (ORCID number 0000-0002-9796-5081)

Email: ondrej.mottl@gmail.com

Address: Department of Biological Sciences, University of Bergen, PO Box 7803, N-5020 Bergen, Norway

Abstract

1. Dynamics in the rate of compositional change beyond the time of human observation are uniquely preserved in palaeoecological sequences from peat or lake sediments. Changes in sedimentation rates and sampling strategies result in an uneven distribution of time intervals within stratigraphical data, which makes assessing rates of compositional change and the detection of periods with a high rate-of-change (RoC) or 'peak-points' challenging. Despite these known issues and their importance, and the frequent use of RoC in palaeoecology, there has been relatively little exploration of differing approaches to quantifying RoC.

2. Here, we introduce R-Ratepol (an easy to use R package) that provides a robust numerical technique for detecting and summarising RoC patterns in complex multivariate time-ordered stratigraphical sequences. We compare the performance of common methods of estimating RoC using simulated pollen-stratigraphical data with known patterns of compositional change and temporal resolution. In addition, we apply our new methodology to four representative European pollen sequences.

3. Simulated data show large differences in the successful detection of known patterns in RoC peak-point detection depending on the smoothing methods and dissimilarity coefficients used, and the level density and their taxonomic richness. Building on these results, we propose a new method of binning with a moving window in combination with a generalised additive model for peak-point detection. The method shows a 22% increase in the correct detection of peak-points and 4% lower occurrence of false positives compared to the more traditional way of peak selection by individual levels, as well as achieving a reasonable compromise between type I and type II errors. The four representative pollen sequences from Europe show that our methodological combination also performs well in detecting periods of significant compositional change including the onset of human activity, early land-use transformation, and changes in fire frequency.

4. Expanding the approach using R-Ratepol to the increasingly available stratigraphical data on pollen, chironomids, or diatoms will allow future palaeoecological and macroecological studies to quantify, and then attribute, major changes in biotic composition across broad spatial areas through time.

KEYWORDS: Compositional change; peak-point detection; pollen analysis; rate-of-change; simulated data

INTRODUCTION

Quantifying spatio-temporal changes in biological composition or diversity is essential for monitoring the current biodiversity crisis and for disentangling underlying drivers like climate, land-use change, pollution, or introduction of invasive species, as well as intrinsic population dynamics driven by biotic interactions (e.g. Wolfe, Champ, Flemer, & Mearns, 1987; Richardson et al., 2006; Silvertown et al., 2006; Gotelli, Dorazio, Ellison, & Grossman, 2010; Magurran et al., 2010; Monchamp et al., 2018; Steinbauer et al., 2018). The importance of such ecological long-term observational studies (50-100 years) is increasingly recognised (Dornelas et al., 2013, 2018; Hillebrand et al., 2018; Magurran, Dornelas, Moyes, & Henderson, 2019). Substantial compositional turnover has been observed during recent decades (e.g. Gibson-Reinemer, Sheldon, & Rahel, 2015; Steinbauer et al., 2018; Feeley, Bravo-Avila, Fadrique, Perez, & Zuleta, 2020) and "The Great Acceleration" following human influences (Steffen, Broadgate, Deutsch, Gaffney, & Ludwig, 2015), either as a result of human impact earlier within the Holocene (Stephens et al., 2019), or in response to regional climate change (Shuman, Bartlein, & Webb, 2005; Seddon, Macias-Fauria, & Willis, 2015). However, similar rates of environmental change may also have occurred in former time periods (Kemp, Eichenseer, & Kiessling, 2015). To understand the impacts of humans on ecosystems it is essential to compare temporal changes in composition and diversity through human history and also to investigate whether such

63 changes are unique to the epoch of human impact ('Anthropocene') or whether they precede human-
64 dominated systems (Birks, Felde, & Seddon, 2016).

65 Palaeoecological sequences of pollen, diatoms, chironomids, cladocerans, etc. preserved in peat or
66 lake sediments are a unique resource for quantifying spatio-temporal changes in biological
67 composition and diversity beyond the time period of human observations. Rate-of-change (RoC)
68 analysis was introduced into palaeoecology by Jacobson and Grimm (1986) to quantify the rate of
69 compositional change and the magnitude of change within a Holocene pollen sequence. It was
70 extended by Jacobson, Webb and Grimm (1987) to quantify and compare rates of change within and
71 between sequences (see also Grimm & Jacobson, 1992) in an attempt to identify regional-scale and
72 local-scale patterns in rates of change. RoC analysis estimates compositional change or temporal beta-
73 diversity between adjacent stratigraphical levels and hence between times. Unlike other estimates of
74 beta-diversity, RoC analysis specifically estimates the magnitude of compositional change per *unit*
75 *time*. Therefore, an essential requirement in RoC analysis is a robust age-depth model for the
76 stratigraphical sequence to precisely estimate the age of levels within the sequence.

77 Despite the wide use of RoC analysis in palaeoecology (e.g. Laird, Fritz, & Cumming, 1998; H. H. Birks
78 & Ammann, 2000; H. J. B. Birks & Birks, 2008; Solovieva, Jones, Birks, Appleby, & Nazarova, 2008;
79 Urrego et al., 2009; Correa-Metrio et al., 2012; Grindean, Tanţău, & Feurdean, 2019; Szabó et al.,
80 2020), there has been relatively little exploration of the underlying methodology of RoC analysis and
81 how the various methodologies and sequence properties influence RoC estimates (but see Lotter,
82 Ammann, & Sturm, 1992; Bennett & Humphry, 1995; Birks, 2012). Different approaches to estimate
83 RoC (Bennett & Humphry, 1995; Birks, 2012) involve choices in terms of approach and technique, such
84 as transforming the stratigraphical levels and associated fossil data (using binning or interpolation to
85 constant time intervals), smoothing the data, and the metric used to estimate the amount of
86 compositional dissimilarity between adjacent levels (Birks, 2012).

87 The variety of approaches available to RoC analysis can, however, create problems. First, Anderson et
88 al. (2020) stress the sensitivity of RoC to temporal sampling variation within and between records,
89 consequently hampering conclusive comparisons. Second, there has been a lack of standardisation
90 between studies (i.e. incorporating different dissimilarity metrics, different temporal procedures)
91 which means that it is not possible to compare RoC between sequences (Birks, 2012). Third, intrinsic
92 properties of an individual sequence, such as its taxonomic richness and the density and distribution
93 of levels within the sequence, can influence the estimated RoC. The end result is that, since the
94 expected patterns of RoC in a sequence are unknown, the most appropriate choices or methods to
95 undertake RoC analysis are also unknown (Bennett & Humphry, 1995; Birks, 2012).

Here, we present a new algorithm for RoC analysis as a standardised and robust methodology, and hence current best practice, for estimating and comparing RoC estimates within and between stratigraphical sequences. Applying our approach, we compare the performance of various methods of estimating RoC using simulated pollen-stratigraphical data (Blaauw, Bennett, & Christen, 2010) with known patterns of compositional change and resolution. We compare results from different smoothing methods and dissimilarity coefficients. In addition, we introduce a method for detecting 'peak-points', defined as a rapid change in taxonomic composition or relative abundances of pollen taxa within the sequence, which provides a means of comparing RoC between sequences and interpreting the potential drivers of assemblage change. We illustrate our approach by estimating RoC values for four palynological sequences with different densities of stratigraphical levels and pollen richness, incorporating age uncertainties from Bayesian age-depth modelling and standardisation of pollen richness. Our approach can provide important information for future palaeoecological and macroecological studies attempting to quantify, and then attribute, major changes in biotic composition across broad spatial areas, and to compare the observed changes in recent decades ('Anthropocene') with changes that occurred within the Holocene (e.g. Gibson-Reinemer et al., 2015).

Materials and Methods

We develop a novel statistical approach to evaluate RoC in a single stratigraphical sequence using pollen-count data and age uncertainties for each level. R-Ratepol is written as an R package (R Core Team 2018). The process of computation in R-Ratepol is summarised in Fig. 1 (a detailed description of each step and all the formulae for the calculations are given in the Supplementary Methods)

Selection of working units

RoC is calculated between consecutive levels or working units (Wus). Traditionally, these Wus represent individual stratigraphical levels. However, changes in sedimentation rates and sampling strategies can result in an uneven distribution of levels within a time sequence, which in turn makes the comparison of RoC between sequences problematic. There are various methods that attempt to minimise such problems. The first is **interpolation of levels** to evenly spaced time intervals, and the use of the interpolated data as WUs. This can lead to a loss of information when the density of levels is high. Second is **binning of levels**: pollen data are pooled into age brackets of various size (bins) and these serve as WUs. Here, the issue is a lower resolution of WUs and their uneven size in terms of total pollen count (bins with more levels have higher pollen counts). Third is **selective binning**. Like classical binning, bins of selected size are created, but instead of pooling pollen data together, only one level is selected as representative of each bin. This results in an even number of WUs in bins with a similar number of pollen grains. However, the issue of low resolution remains.

We propose **a new method of binning with a moving window**, which is a compromise between using individual levels and selective binning. This method follows a simple sequence: bins are created, levels are selected as in selective binning, and RoC between bins is calculated. However, the brackets of the time bin (window) are then moved forward by a selected amount of time (Z), levels are selected again, and RoC calculated for the new set of WUs. This is repeated X times (where X is the bin size divided by Z) while retaining all the results (See Fig. 1 and the Supplementary Methods).

Simulated data

We simulated pollen datasets following Blaauw *et al.* (2010) based on generating pollen-assemblage data in response to known changes in environmental conditions and compositional properties (Fig. S1). The settings in the simulation algorithm were changed according to: i) richness – *low richness* (LR) datasets contain 5 pollen taxa, *high richness* (HR) datasets contain 50 pollen taxa; and ii) position of change in external environmental properties – *recent* (R) has a sudden increase of environmental properties at 2000 calibrated years before present (1950 CE: cal yr BP) and a decrease at 3000 cal yr BP, *late* (L) has a sudden increase at 5500 and a decrease at 6500 cal yr BP (Fig. S1). This results in two abrupt changes in pollen composition in each dataset. Note that the different timings of the change in environmental properties (hereafter called 'focal area') were selected to illustrate the effects of level density (datasets with the *later* manual edit have a low density of levels within the focal area and datasets with a *recent* manual edit have a high density). The combination of these two settings results in four types of simulated datasets: *low richness – recent change* (LR-R)*, low richness – late change* (LR-L)*, high richness – recent change* (HR-R), and *high richness – late change* (HR-L). To increase the reliability of the simulated data, we used the density of levels from a European pollen sequence, Glendalough (Sequence A) as a template for the number of levels and their corresponding ages to each level. We then adjusted the total values of each simulated taxon so that the pollen assemblage resembles a log-scale rank distribution and added jitter to each of the pollen taxa (function *jitter*, factor = 1.5).

Using the simulated datasets to test analytical performance with different settings

Using R-Ratepol, we implemented three types of WU selection (individual stratigraphical levels, selective binning, and binning with moving window), five types of smoothing of pollen data (none, moving average, Grimm's smoothing (Grimm & Jacobson, 1992), age-weighted average, Shepard's 5-term filter (Davis, 1986; Wilkinson, 2005)), four types of dissimilarity coefficient (Euclidean distance, standardised Euclidean distance, Chord distance, Chi-squared coefficient (Prentice, 1980)), and three types of peak-point detection (Threshold, generalised additive model (GAM), Signal-to-Noise Index (SNI; Kelly, Higuera, Barrett, & Feng Sheng, 2011)). In order to investigate the differences between the various settings, we used the four types of simulated datasets (LR-R, LR-L, HR-R, HR-L; see above),

simulated 100 datasets for each dataset type, and compared the success rate of detecting peak-points in the expected time period for all combinations of WU selection, smoothing type, dissimilarity coefficient, and peak-point detection.

To detect significant peak-points of RoC scores in each sequence, each point is tested to see if it represents a significant increase in RoC values (the criteria vary between the peak-point detection methods, see Supplementary Methods for details). For all simulated datasets with all WU selections, smoothing, and dissimilarity coefficient combinations, we extracted a) the number of WUs where R-Ratepol detects a significant peak-point during the focal area (± 500 yr), and b) the number of samples, where R-Ratepol detects a peak-point during a time of no expected change ('false positives'). First, we test if the various WU selection methods affect the successful detection of peak-points within the focal area. We pooled all randomisations from all dataset types and created generalised linear mixed models using the Template Model Builder (Brooks et al., 2017) $\mathrm{glmmTMB}_{success-method}$ with the ratio of levels marked as peak-points to all levels in the focal area ($R_{success-method}$) as the dependent variable with a beta-binomial error distribution. Independent variables were: WU (3 level factor), peak-point detection method (3 level factor), position of environmental change (i.e. density of levels; 2 level factor), richness of dataset (2 level factor), and all their interactions. Individual dataset ID was selected as the random factor. We then used the *dredge* function from the *MuMIn* package (Barton, 2020) to reduce unnecessary predictors using a test of parsimony (AICc). We used the *emmens* package (Russell, 2020) to obtain estimated marginal means and the 95% quantile of the independent variables from the final model. Similarly, we built $\mathrm{glmmTMB}_{FalsePositive-method}$ using the ratio of WU marked as peak-points to all WU outside the focal area ($R_{FalsePositives-method}$).

Next, for more a detailed exploration of different settings in R-Ratepol, we divided the data to only include the best performing WU selection and peak-point detection combination (i.e. binning with moving window and GAM peak-point detection, see Results) and created $\mathrm{glmmTMB}_{success-settings}$ and $\mathrm{glmmTMB}_{FalsePositive-settings}$ with $R_{success-settings}$ and $R_{FalsePositives-settings}$ as the dependent variables, respectively. Both models were fitted with a beta-binomial error distribution and the independent variables were data-smoothing type (5 level factor), dissimilarity coefficient (4 level factor), position of environmental change (i.e. density of levels; 2 level factor), richness of dataset (2 level factor), and all their interactions. Individual dataset ID was selected as the random factor. The *dredge* function was used to reduce unnecessary predictors.

Examples of rate-of-change results using real palynological data

After assessing the differences between the individual settings of R-Ratepol based on the results from the simulated datasets, we examined the RoC score for real palynological data representing different

196 pollen richness and composition, and different density of levels. We obtained pollen data from the
197 Neotoma database (Williams, Grimm, et al., 2018) using the *Neotoma R package* (Goring et al., 2015).
198 We chose four European sequences (A–D; Fig 2). Taxa were standardised to the taxonomically highest
199 pollen morphotype (Level = MHVar2) using the pollen harmonisation table in Giesecke et al. (2019).

200 To develop age-depth models, we used the pre-selected radiometric control points provided in
201 Giesecke et al. (2014) and calibrated the radiocarbon dates using the IntCal13 Northern Hemisphere
202 calibration curve (Reimer et al., 2013). For each sequence, we constructed an age-depth model using
203 the *Bchron* R package (Haslett & Parnell, 2008) to generate 1000 possible age predictions (i.e. age
204 uncertainties) for all levels. We calculated the median of all the uncertainties for each level to give the
205 most probable age (default age) in cal yr BP.

206 In each sequence, we excluded all levels that contained less than 150 pollen counts of terrestrial taxa,
207 and all levels beyond a 3000-years extrapolation of the oldest chronological control point. In addition,
208 we excluded all levels with an age older than 8500 cal yr BP to ensure focus on the period with
209 substantial human impact.

210 **Sequence A** is from Glendalough, Ireland (53°00’10.0"N 6°22’09.0"W; Haslett et al., 2006). It has a
211 very uneven distribution of levels (N = 101) with the highest density around 2000 cal yr BP (Fig. 2A).
212 The sequence contains 80 pollen taxa with abundant *Corylus*, *Quercus, Alnus, Betula*, and Poaceae.
213 Cyperaceae, Poaceae, and Ericales all increase in the last 1000 cal yr BP, preceded by a period with
214 high values of *Quercus*, *Betula*, and *Alnus* until ~ 5000 cal yr BP. Before 5000 cal yr BP the sequence
215 has large variations in *Pinus*, an increase of *Alnus*, and a large decrease in *Corylus*. **Sequence B** is from
216 Dallican Water, Scotland (60°23’14.5"N 1°05’47.3"W; Bennett, Boreham, Sharp, & Switsur, 1992). It
217 has a relatively even distribution of levels (N = 60; Fig. 2B) and contains 50 pollen taxa with Ericales,
218 *Betula*, and Poaceae being the most abundant. The pollen record shows sudden increases of Ericales
219 after 4000 cal yr BP. **Sequence C** is from Steerenmoos, Germany (47°48’20.0"N 8°12’01.6"E; Rösch,
220 2000). It is an example of a very detailed sequence, but with an uneven distribution of levels (N = 256;
221 Fig. 2C). The sequence contains 103 pollen taxa with *Abies*, *Fagus*, *Corylus, Betula*, and *Quercus* being
222 the most abundant. As with Sequence A, the pollen stratigraphy can be separated into three major
223 parts: i) a recent period until 1000 cal yr BP typified by high values of *Pinus*; ii) 2000–6000 cal yr BP
224 typified by *Abies* and *Fagus*; and iii) 6000 cal yr BP to the base with abundant *Betula*, *Corylus*, and
225 *Quercus*. **Sequence D** is from Alanen Laanijärvi, a boreal-forest lake in Swedish Lapland (67°58’00.9"N
226 20°27’37.9"W; Heinrichs, Peglar, Bigler, & Birks, 2005). It is an example of a sequence with 54 levels
227 across the time of interest, containing 44 pollen taxa with high values of *Pinus* and *Betula* throughout
228 the whole sequence (Fig. 2D).

We calculated RoC scores for the four selected European sequences (A-D) using all three methods of WU selection with age-weighted average smoothing and Chi-squared coefficient selected as the dissimilarity coefficient. A GAM approach was used for detecting peak-points in each sequence, the number of randomisations was set to 10,000, and the size of time bin was selected as 500 yr (see Fig. S2 for example of changes of RoC values with size of time bin). In addition, to provide examples of the differences between different settings of R-Ratepol, we explored data from sequence A using binning with the moving window method of WU selection and calculated RoC scores for all data smoothing and dissimilarity coefficient combinations.

RESULTS

Comparison of success rates in peak-point detection for simulated datasets

Successful detection of peak-points ($R_{success-method}$) and the number of incorrectly (false positives) detected peak-points ($R_{FalsePositives-method}$) are both significantly affected by WU selection, method of peak-point detection, density of levels in the sequence, and taxonomic richness of the dataset (Fig. 3A; see Table S1 and Table S2 for the best selected models). For detecting peak-points successfully within the focal area, the GAM method scores relatively highly (estimated marginal means are 60% higher than the SNI method; Fig. 3A), and with a relatively low false positive rate compared to the other peak-point detection methods (estimated marginal means are 40% lower than the threshold method; Fig. 3A). Simulations show that using our approach of binning with a moving window results in an overall better performance in successful peak-point detection than selective binning or the use of individual levels (Fig. 3). The GAM method has 20 and 22% higher marginal means of success detection than selective binning and the use of individual levels, respectively.

While using only the binning with the moving-window approach and the GAM method for peak-point detection, the successful detection of peak-points ($R_{success-settings}$) and the number of false positives ($R_{FalsePositives-settings}$) are both influenced by the density of levels, dataset richness, type of dissimilarity coefficient, and data-smoothing type (Fig. 3B; see Tables S3 and S4 for the best selected models). The datasets with recent environmental change (i.e. change in the time of high density of levels) show estimated marginal means with a 28% higher success of peak-point detection and 3% lower false positive detection than datasets with environmental change later in the sequence (i.e. change at the time of low density of levels; Fig. S3). Datasets with a high richness of pollen taxa have estimated marginal means with a 5% higher success in the detection of peak-points than datasets with low richness (Fig. S3). Datasets using the Chi-squared coefficient as the dissimilarity coefficient have the highest number of correctly detected peak-points (3% higher estimated marginal means than the second best, Chord distance; Fig. S3). All smoothing types show similar results, except Grimm's

smoothing, which has the lowest success in the correct detection of peak-points and the highest number of false positives compared to other smoothers (Fig. S3).

Examples of rate-of-change results using real palynological data

The selection of WUs affected not only the overall shape of the RoC curve in all sequences but also the timing of the period of significant increase in the RoC (Fig. 2). Binning with a moving window detected significant periods of increased RoC scores at sequence A (Glendalough) between 4200–5000 cal yr BP; sequence B (Dallican Water) between 3200–3500 cal yr BP; sequence C (Steerenmoos) between 5800–6400 cal yr BP; and sequence D (Alanen Laanijärvi) between 350–580 cal yr BP (Fig. 2). These patterns remain relatively similar with selective binning but not when individual levels are used as WUs.

Discussion

Based on the results of our simulations, the choice of methods and parameters is critical in the analysis of rate-of-change in pollen sequences. Comparison of methods using simulated datasets shows that selection of WUs, peak-point detection method, dissimilarity coefficient, smoothing of the data, density of the levels in the period of environmental change, and pollen richness significantly influence the detection of sudden changes in stratigraphical sequences. Our proposed method of binning with a moving window in combination with GAM peak-point detection improves the detection of increased RoC. The method shows a 22% increase in the correct detection of peak-points and a 4% lower occurrence of false positives compared to the more traditional approach of selection by individual levels. Peak-point detection using GAM provides a reasonable compromise between statistical error type I (*Threshold* method) and type II (*SNI* method).

Using the Chi-squared coefficient as the dissimilarity coefficient shows overall the best results, and we therefore recommend using this measure for palaeoecological data sequences that are expressed as percentages or proportions. Recommendation of a specific smoothing technique of data is less straightforward. There is a trade-off between the degree of smoothing of the data and the density of samples in the expected period of higher RoC. For example, Shepard's 5-term filter (relatively soft smoothing of data) and data without smoothing do not perform well in the specific case where environmental change occurred during the period with a low density of samples. Detailed exploration of the RoC pattern in sequence A (Fig. 4) shows that all smoothing methods detected the RoC increase in the period between 4000–6000 cal yr BP but also others in the recent period (0–500 yr BP). The latter are likely to be false positives as this period is characterised by a low density of levels and used Shepard's 5-term filter data smoothing. Smoothing using age-weighted average is able to perform better in such a scenario but at the cost of an increased number of false positives. Therefore, there is

a need for critical evaluation in future studies to assess the risks of using either Shepard's 5-term filter or age-weighted average data for smoothing, depending on the research questions of interest.

A multitude of appropriate data-smoothing approaches (Wilkinson, 2005), dissimilarity coefficients (e.g. Prentice, 1980; Legendre & Legendre, 2012), techniques for creating working units, and methods of peak-point detection (e.g. Simpson, 2018) are potentially available. Of the four selected dissimilarity methods and four smoothing algorithms, all commonly used in palaeoecology, we conclude that datasets with a high density of levels tend to have a higher chance of successfully detecting peak-points. Anderson et al. (2020) reached similar conclusions in a regional-scale synthesis of fossil pollen data from California. Here the authors suggest maintaining a consistent temporal spacing within records, and the use of probabilistic models explicitly incorporating age-model uncertainties to increase the precision of age estimates of each level. We show that our method of binning with a moving window yields better results than the traditional selective binning method. Using R-Ratepol is an advantage in this case as such age-model uncertainties can be incorporated.

RoC analysis has several applications in palaeoecological research. It is a useful numerical tool to detect patterns in stratigraphical data that cannot readily be seen by visual inspection (see Jacobson et al., 1987 for an example at Gould Pond, Maine). It is also useful to compare the rates of change in different proxies (e.g. pollen, diatoms, chironomids, etc.) studied in the same stratigraphical sequence (e.g. Birks & Ammann, 2000; Szabó et al., 2020). Moreover, it is most useful when RoC results are compared from several sequences (e.g. Jacobson et al., 1987; Grimm & Jacobson, 1992). Consistent patterns in RoC peaks in several sequences may potentially indicate response to extrinsic drivers such as regional climate change, pathogenic attacks, or widespread human activity. Ecologists are recognising the importance of quantifying RoC of extrinsic drivers such as temperature, toxins, and salinity on ecosystems (Pinek et al., 2020) and are developing new and powerful numerical tools for space–time analysis of community compositional data over time intervals of decades (e.g. Legendre & Gauthier, 2014). RoC peaks unique to individual sequences may, in contrast, reflect local factors such as sequence hiatuses, sedimentary reworking, or spatially restricted human impact or disturbance.

A connection between RoC and local factors can be seen in sequences used in this study (Fig. 2). Sequence A (Glendalough) shows significant peak-points at the time of the onset of human activity and the expansion of grassland and heath (Haslett et al., 2006). Sequence B (Dallican Water) has significant peak-points at times when major changes in land-use occurred as the island was abandoned by humans and then reinhabited 800 years later (Bennett et al., 1992). Sequence C (Steerenmoos) has several significant peak-points at the time of the expansion of *Abies* pollen in the late Neolithic period

and with frequent fires (Rösch, 2000). Sequence D (Alanen Laanijärvi) has significant peak-points in the very recent period, possibly associated with changes in organic deposition, fertilisation, and timber harvesting (Heinrichs et al., 2005). Here we can assume that our approach of binning with a moving window is closest to the expected pattern, further supported by the relatively high detection of peak-points in the simulated datasets (Fig. 3). In contrast, the traditional use of individual levels fails to detect the period of significant change (5800–6400 cal yr BP) in sequence C, or falsely assigns peak-points to other, non-relevant periods (sequence A: 2000 cal yr BP; sequence C; 0–500 cal yr BP; sequence D: 0–4000 cal yr BP), or a combination of both (sequence B). Most of these errors occur, as expected, with low density sample levels. These sequences and the RoC outcomes exemplify the usefulness of quantifying rates of compositional change estimated through time.

In summary, we have developed a framework for the robust estimation of rate-of-change in stratigraphical time-ordered palaeoecological sequences of, for example, pollen, chironomids, or diatoms. Our overall framework consists of four major parts:

1. Establishing a robust age-depth model for the stratigraphical sequence of interest with age uncertainties for all individual levels.
2. Selecting consecutive working units prior to RoC estimation to allow for uneven temporal distribution of the analysed levels within the sequence using selective binning with a moving window.
3. Estimating compositional dissimilarity between working units.
4. Detecting statistically significant peak-points in the RoC estimates within the sequence.

RoC analysis as implemented in R-Ratepol is a significant advance over existing methods for RoC analysis that do not incorporate methods to detect statistically significant peak-points (Birks, 2012). R-Ratepol is, we believe, a useful addition to the toolkit of robust numerical techniques available to palaeoecologists and palaeolimnologists for detecting and summarising patterns in complex multivariate time-ordered stratigraphical sequences (Birks, 2010).

Acknowledgements

All the authors are supported by the European Research Council under the EU Horizon 2020 Research and Innovation Programme (grant 741413 HOPE) Humans on Planet Earth – Long-term impacts on biosphere dynamics. HJBB is indebted to John Line (University of Cambridge) for collaboration in 1990 in the development of the Fortran77 RATEPOL program, which was a starting point for R-Ratepol, to Cathy Jenks for indispensable editorial help, and to Hilary Birks for many helpful discussions. Data were obtained from the Neotoma Paleoecology Database (www.neotoma.org) and its constituent

European Pollen Database (EPD). The work of the data contributors, data stewards, and the Neotoma and EPD community is gratefully acknowledged.

AUTHORS' CONTRIBUTION

OM and HJBB conceived the ideas and designed the study. OM led the manuscript writing, analyses and interpretation of the data. OM, AWRS, KPB, VAF, and SGAF designed the methodology for extracting and processing palaeoecological sequences from Neotoma. OM, JAG, AWRS, MJS, and HJBB contributed to methodology development. HJBB acquired the funding. All authors contributed to the writing of the text and interpretation of the results and gave final approval for publication.

DATA AVAILABILITY

R-Ratepol is available as an R package at GITHUB (https://github.com/HOPE-UIB-BIO/R-Ratepol-package), including all the data used in this study. Script for all analyses used in this study can be found at GITHUB repository (https://github.com/HOPE-UIB-BIO/RateOfChange).

REFERENCES

Anderson, L., Wahl, D. B., & Bhattacharya, T. (2020). Understanding rates of change: A case study using fossil pollen records from California to assess the potential for and challenges to a regional data synthesis. Quaternary International. doi:10.1016/j.quaint.2020.04.044

Barton, K. (2020). MuMIn: Multi-Model Inference. R package version 1.43.17.

Bennett, K. D., Boreham, S., Sharp, M. J., & Switsur, V. R. (1992). Holocene history of environment, vegetation and human settlement on Catta Ness, Lunnasting, Shetland. Journal of Ecology, 80(2), 241. doi:10.2307/2261010

Bennett, K. D., & Humphry, R. W. (1995). Analysis of late-glacial and Holocene rates of vegetational change at two sites in the British Isles. Review of Palaeobotany and Palynology, 85(3–4), 263–287. doi:10.1016/0034-6667(94)00132-4

Birks, H. H., & Ammann, B. (2000). Two terrestrial records of rapid climatic change during the Glacial-Holocene Transition (14,000–9,000 calendar years B.P.) from Europe. Proceedings of the National Academy of Sciences of the United States of America, 97(4), 1390–1394.

Birks, H. J. B. (2010). Numerical methods for the analysis of diatom assemblage data. In J. P. Smol & E. F. Stoermer (Eds.), The diatoms: applications for the environmental and earth sciences (2nd edn., pp. 23–54). Cambridge University Press, Cambridge.

Birks, H. J. B. (2012). Analysis of stratigraphical data. In H. J. B. Birks, A. F. Lotter, S. Juggins, & J. P. Smol (Eds.), Tracking Environmental Change Using Lake Sediments Volume 5: Data Handling and Numerical Techniques (pp. 355-378). Dordrecht: Springer.

Birks, H. J. B., & Birks, H. H. (2008). Biological responses to rapid climate change at the Younger Dryas-Holocene transition at Kråkenes, western Norway. The Holocene, 18(1), 19–30. doi:10.1177/0959683607085572

Birks, H. J. B., Felde, V. A., & Seddon, A. W. R. (2016). Biodiversity trends within the Holocene. The Holocene, 26(6), 994–1001. doi:10.1177/0959683615622568

Blaauw, M., Bennett, K. D., & Christen, J. A. (2010). Random walk simulations of fossil proxy data. The Holocene, 20(4), 645–649. doi:10.1177/0959683609355180

Brooks, M. E., Kristensen, K., van Benthem, K. J., Magnusson, A., Berg, C. W., Nielsen, A., & Skaug, H. J. (2017). glmmTMB Balances Speed and Flexibility Among Packages for Zero-inflated Generalized Linear Mixed Modeling. The R Journal, 9(2), 378–400. doi:10.3929/ethz-b-000240890

403 Correa-Metrio, A., Bush, M. B., Cabrera, K. R., Sully, S., Brenner, M., Hodell, D. A., … Guilderson, T.
404 (2012). Rapid climate change and no-analog vegetation in lowland Central America during the
405 last 86,000 years. Quaternary Science Reviews, 38, 63–75. doi:10.1016/j.quascirev.2012.01.025

406 Davis, J. C. (1986). Statistics and Data Analysis in Geology (2nd edn.). J. Wiley & Sons, New York.

407 Dornelas, M., Magurran, A. E., Buckland, S. T., Chao, A., Chazdon, R. L., Colwell, R. K., … Vellend, M.
408 (2013). Quantifying temporal change in biodiversity: Challenges and opportunities. Proceedings
409 of the Royal Society B: Biological Sciences, 280(1750), 20121931. doi:10.1098/rspb.2012.1931

410 Dornelas, M., Antão, L. H., Moyes, F., Bates, A. E., Magurran, A. E., Adam, D., ... Zettler, M. L. (2018).
411 BioTIME: A database of biodiversity time series for the Anthropocene. Global Ecology and
412 Biogeography, 27(7), 760-786. doi:10.1111/geb.12729

413 Feeley, K. J., Bravo-Avila, C., Fadrique, B., Perez, T. M., & Zuleta, D. (2020). Climate-driven changes in
414 the composition of New World plant communities. Nature Climate Change.
415 doi:10.1038/s41558-020-0873-2

416 Gibson-Reinemer, D. K., Sheldon, K. S., & Rahel, F. J. (2015) Climate change creates rapid species
417 turnover in montane communities. Ecology and Evolution, 5(12), 2340-2347.
418 doi:10.1002/ece3.1518

419 Giesecke, T., Davis, B., Brewer, S., Finsinger, W., Wolters, S., Blaauw, M., … Bradshaw, R. H. W. (2013).
420 Towards mapping the late Quaternary vegetation change of Europe. Vegetation History and
421 Archaeobotany, 23(1), 75–86. doi:10.1007/s00334-012-0390-y

422 Giesecke, T., Wolters, S., van Leeuwen, J. F. N., van der Knaap, P. W. O., Leydet, M., & Brewer, S.
423 (2019). Postglacial change of the floristic diversity gradient in Europe. Nature Communications,
424 10(1). doi:10.1038/s41467-019-13233-y

425 Goring, S., Dawson, A., Simpson, G. L., Ram, K., Graham, R. W., Grimm, E. C., & Williams, J. W. (2015).
426 Neotoma: A programmatic interface to the Neotoma paleoecological database. Open
427 Quaternary, 1, 1–17. doi:10.5334/oq.ab

428 Gotelli, N. J., Dorazio, R. M., Ellison, A. M., & Grossman, G. D. (2010). Detecting temporal trends in
429 species assemblages with bootstrapping procedures and hierarchical models. Philosophical
430 Transactions of the Royal Society B: Biological Sciences, 365(1558), 3621–3631.
431 doi:10.1098/rstb.2010.0262

432 Grimm, E. C., & Jacobson, G. L. (1992). Fossil-pollen evidence for abrupt climate changes during the
433 past 18000 years in eastern North America. Climate Dynamics, 6, 179–184.

434 Grindean, R., Tanţău, I., & Feurdean, A. (2019). Linking vegetation dynamics and stability in the old-
435 growth forests of Central Eastern Europe: Implications for forest conservation and
436 management. Biological Conservation, 229, 160–169. doi:10.1016/j.biocon.2018.11.019

437 Haslett, J., & Parnell, A. (2008). A simple monotone process with application to radiocarbon-dated
438 depth chronologies. Journal of the Royal Statistical Society. Series C: Applied Statistics, 57(4),
439 399–418. doi:10.1111/j.1467-9876.2008.00623.x

440 Haslett, J., Whiley, M., Bhattacharya, S., Salter-Townshend, M., Wilson, S. P., Allen, J. R. M., … Mitchell,
441 F. J. G. (2006). Bayesian palaeoclimate reconstruction. Journal of the Royal Statistical Society.
442 Series A: Statistics in Society, 169(3), 395–438. doi:10.1111/j.1467-985X.2006.00429.x

443 Heinrichs, M., Peglar, S. M., Bigler, C., & Birks, H. J. B. (2005). A multi-proxy palaeoecological study of
444 Alanen Laanijärvi, a boreal-forest lake in Swedish Lapland. Boreas, 34(2), 192–206.
445 doi:10.1080/03009480510012881

446 Hillebrand, H., Blasius, B., Borer, E. T., Chase, J. M., Downing, J. A., Eriksson, B. K., … Ryabov, A.B.
447 (2018). Biodiversity change is uncoupled from species richness trends: Consequences for
448 conservation and monitoring. Journal of Applied Ecology, 55, 169-184. 10.1111/1365-
449 2664.12959

450 Jacobson, G. L., & Grimm, E. C. (1986). A numerical analysis of Holocene forest and prairie vegetation
451 in Central Minnesota. Ecology, 67(4), 958–966.

452 Jacobson, G. L., Webb, T., & Grimm, E. C. (1987). Patterns and rates of vegetation change during the
453 deglaciation of eastern North America. In W. F. Ruddiman & H. E. Wright (Eds.), North America
454 and Adjacent Oceans During the Last Deglaciation (pp. 277–288). Geological Society of America,
455 Boulder, Colorado. doi:10.1130/dnag-gna-k3.277

456 Kelly, R. F., Higuera, P. E., Barrett, C. M., & Feng Sheng, H. (2011). A signal-to-noise index to quantify
457 the potential for peak detection in sediment-charcoal records. Quaternary Research, 75(1), 11–
458 17. doi:10.1016/j.yqres.2010.07.011

459 Kemp, D. B., Eichenseer, K., & Kiessling, W. (2015). Maximum rates of climate change are
460 systematically underestimated in the geological record. Nature Communications, 6, 1–6.
461 doi:10.1038/ncomms9890

462 Laird, K. R., Fritz, S. C., & Cumming, B. F. (1998). A diatom-based reconstruction of drought intensity,
463 duration, and frequency from Moon Lake, North Dakota: A sub-decadal record of the last 2300
464 years. Journal of Paleolimnology, 19(2), 161–179. doi:10.1023/A:1007929006001

Legendre, P., & Gauthier, O. (2014). Statistical methods for temporal and space–time analysis of community composition data. Proceedings of the Royal Society B: Biological Sciences, 281(1778), 20132728. doi:10.1098/rspb.2013.2728

Legendre, P., & Legendre, L. (2012). Numerical ecology (3rd English edn.). Elsevier, Amsterdam. doi:10.1016/B978-0-12-409548-9.10595-0

Lotter, A. F., Ammann, B., & Sturm, M. (1992). Rates of change and chronological problems during the late-glacial period. Climate Dynamics, 6(3–4), 233–239. doi:10.1007/BF00193536

Magurran, A. E., Baillie, S. R., Buckland, S. T., Dick, J. M. P., Elston, D. A., Scott, E. M., … Watt, A. D. (2010). Long-term datasets in biodiversity research and monitoring: Assessing change in ecological communities through time. Trends in Ecology and Evolution, 25(10), 574–582. doi:10.1016/j.tree.2010.06.016

Magurran, A. E., Dornelas, M., Moyes, F., & Henderson, P. A. (2019). Temporal β diversity—A macroecological perspective. Global Ecology and Biogeography, 28(12), 1949-1960. doi:10.1111/geb.13026

Monchamp, M. E., Spaak, P., Domaizon, I., Dubois, N., Bouffard, D., & Pomati, F. (2018). Homogenization of lake cyanobacterial communities over a century of climate change and eutrophication. Nature Ecology and Evolution, 2(2), 317–324. doi:10.1038/s41559-017-0407-0

Pinek, L., Mansour, I., Lakovic, M., Ryo, M., & Rillig, M. C. (2020). Rate of environmental change across scales in ecology. Biological Reviews. doi:10.1111/brv.12639

Prentice, I. C. (1980). Multidimensional scaling as a research tool in Quaternary palynology: A review of theory and methods. Review of Palaeobotany and Palynology, 31(C), 71–104. doi:10.1016/0034-6667(80)90023-8

R Core Team. (2018). R: A language and environment for statistical computing. Vienna, Austria: R Foundation for Statistical Computing.

Reimer, P. J., Bard, E., Bayliss, A., Beck, J. W., Blackwell, P. G., Ramsey, C. B., … van der Plicht, J. (2013). IntCal13 and Marine13 radiocarbon age calibration curves 0–50,000 years cal BP. Radiocarbon, 55(4), 1869–1887. doi:10.2458/azu_js_rc.55.16947

Richardson, A. J., Walne, A. W., John, A. W. G., Jonas, T. D., Lindley, J. A., Sims, D. W., … Witt, M. (2006). Using continuous plankton recorder data. Progress in Oceanography, 68(1), 27–74. doi:10.1016/j.pocean.2005.09.011

495 Rösch, M. (2000). Long-term human impact as registered in an upland pollen profile from the southern
496 Black Forest, south-western Germany. Vegetation History and Archaeobotany, 9(4), 205–218.
497 doi:10.1007/BF01294635

498 Russell, L. (2020). emmeans: Estimated Marginal Means, aka Least-Squares Means. R package version
499 1.4.8.

500 Seddon, A. W. R., Macias-Fauria, M., & Willis, K. J. (2015). Climate and abrupt vegetation change in
501 Northern Europe since the last deglaciation. The Holocene, 25(1), 25–36.
502 doi:10.1177/0959683614556383

503 Shuman, B., Bartlein, P. J., & Webb, T. (2005). The magnitudes of millennial- and orbital-scale climatic
504 change in eastern North America during the Late Quaternary. Quaternary Science Reviews,
505 24(20–21), 2194–2206. doi:10.1016/j.quascirev.2005.03.018

506 Silvertown, J., Poulton, P., Johnston, E., Edwards, G., Heard, M., & Biss, P. M. (2006). The Park Grass
507 Experiment 1856-2006: Its contribution to ecology. Journal of Ecology, 94(4), 801–814.
508 doi:10.1111/j.1365-2745.2006.01145.x

509 Simpson, G. L. (2018). Modelling palaeoecological time series using generalised additive models.
510 Frontiers in Ecology and Evolution, 6, 1–21. doi:10.3389/fevo.2018.00149

511 Solovieva, N., Jones, V., Birks, H. J. B., Appleby, P. G., & Nazarova, L. (2008). Diatom responses to 20th
512 century climate warming in lakes from the northern Urals, Russia. Palaeogeography,
513 Palaeoclimatology, Palaeoecology, 259(2–3), 96–106. doi:10.1016/j.palaeo.2007.10.001

514 Steffen, W., Broadgate, W., Deutsch, L., Gaffney, O., & Ludwig, C. (2015). The trajectory of the
515 Anthropocene: The Great Acceleration. Anthropocene Review, 2(1), 81–98.
516 doi:10.1177/2053019614564785

517 Steinbauer, M. J., Grytnes, J.-A., Jurasinski, G., Kulonen, A., Lenoir, J., Pauli, H., … Wipf, S. (2018).
518 Accelerated increase in plant species richness on mountain summits is linked to warming.
519 Nature, 556(7700), 231–234. doi:10.1038/s41586-018-0005-6

520 Stephens, L., Fuller, D., Boivin, N., Rick, T., Gauthier, N., Kay, A., … Ellis, E. (2019). Archaeological
521 assessment reveals Earth's early transformation through land use. Science, 365(6456), 897–
522 902. doi:10.1126/science.aax1192

523 Szabó, Z., Buczkó, K., Haliuc, A., Pál, I., L. Korponai, J., Begy, R.-C., ... Magyari, E. K. (2020). Ecosystem
524 shift of a mountain lake under climate and human pressure: A move out from the safe operating
525 space. Science of the Total Environment, 743, 140584. doi:10.1016/j.scitotenv.2020.140584

526 Urrego, D. H., Bush, M. B., Silman, M. R., Correa-Metrio, A. Y., Ledru, M.-P., Mayle, F. E., … Valencia,
527 B. G. (2009). Millennial-scale ecological changes in tropical South America since the Last Glacial
528 Maximum. In F. Vimeaux, F. Sylvestre, & M. Khodri (Eds.), Past Climate Variability in South
529 America and Surrounding Regions (pp. 283–300). Springer, Dordrecht. doi:10.1007/978-90-481-
530 2672-9_12

531 Wilkinson, L. (2005). The Grammar of Graphics. Springer-Verlag, New York, USA 37.
532 doi:10.2307/2669493

533 Williams, J. W., Grimm, E. C., Blois, J. L., Charles, D. F., Davis, E. B., Goring, S. J., ... Takahara, H. (2018).
534 The Neotoma Paleoecology Database, a multiproxy, international, community-curated data
535 resource. Quaternary Research, 89(1), 156-177. doi:10.1017/qua.2017.105

536 Wolfe, D. A., Champ, M. A., Flemer, D. A., & Mearns, A. J. (1987). Long-term biological data sets: Their
537 role in research, monitoring, and management of estuarine and coastal marine systems.
538 Estuaries, 10(3), 181–193. doi:10.2307/1351847

539 FIGURES AND TABLES

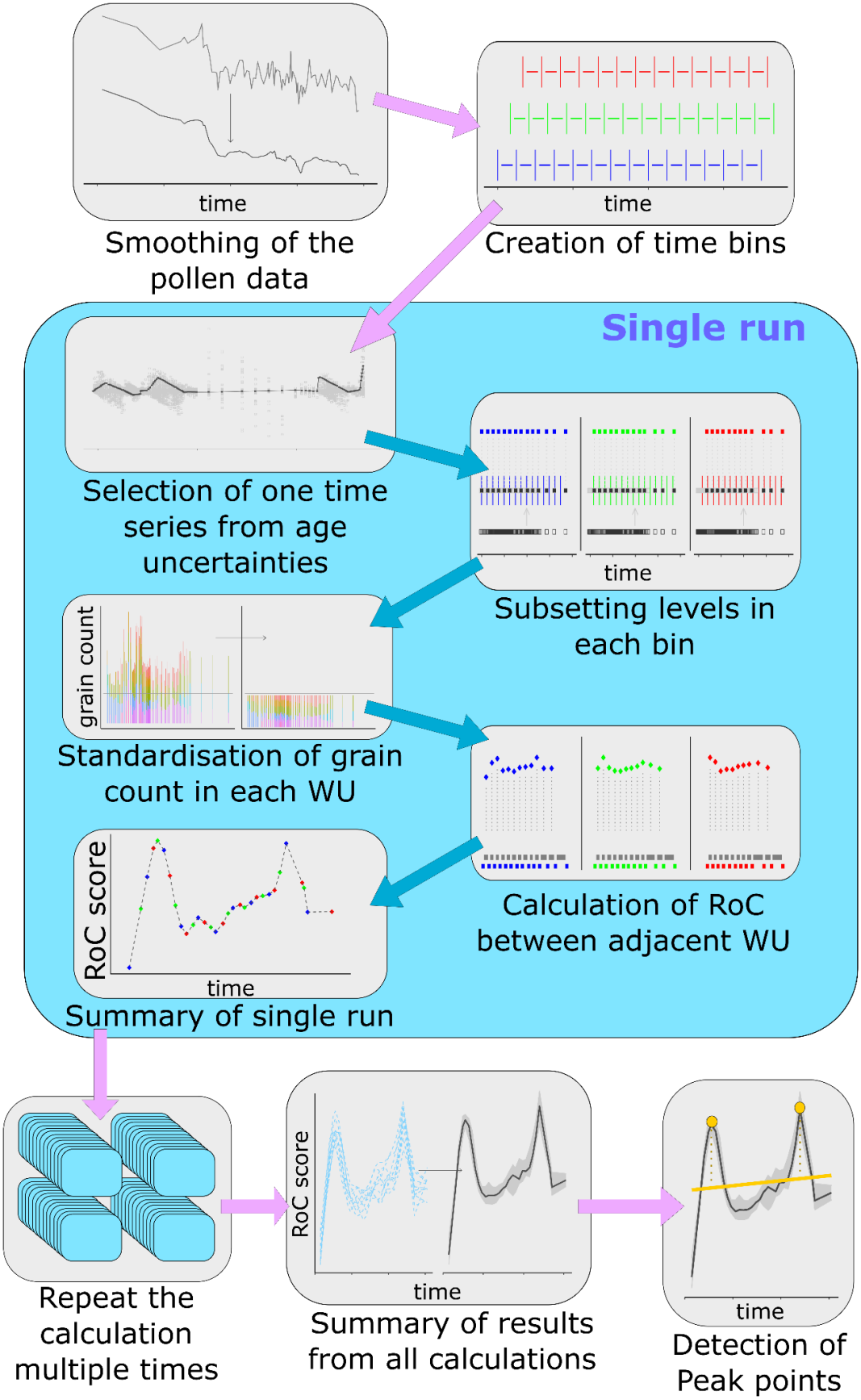

540

Figure 1. Schematic visualisation of R-Ratepol calculation with binning with a moving window.

1) Smooth pollen data (smooth each taxon using one of five selected smoothing methods: *none*, *moving average*, *Grimm's smoothing*, *age-weighted average*, or *Shepard's 5-term filter*.
2) Create template for all bin brackets in all window movements.
3) Steps in each single run (an individual loop):
    a. Randomly select a single age sequence from age uncertainties for all levels
    b. Create working units (WUs) (i.e. subsetting levels in each bin)
    c. (optional) Data standardisation (subsampling pollen data in each WU to a total count of 150 pollen grains).
    d. Calculate the RoC as the dissimilarity coefficient (DC) between adjacent WUs (four different dissimilarity coefficients: *Euclidean distance*, *standardised Euclidean distance*, *Chord distance*, *Chi-squared coefficient*) standardised by age differences between WUs.
    e. Summary of RoC results from all moving windows
4) Repeat the run multiple times (default = 10,000)
5) Validate and summarise results from all runs; exclude data from beyond the selected time period (i.e. 8000 cal yr BP in this study).
6) Detect and validate significant peak-points (three ways of testing for the significance of individual RoC points: *Threshold*, *Generalised Additive Model* (GAM), and *Signal-to-Noise Index* (SNI).

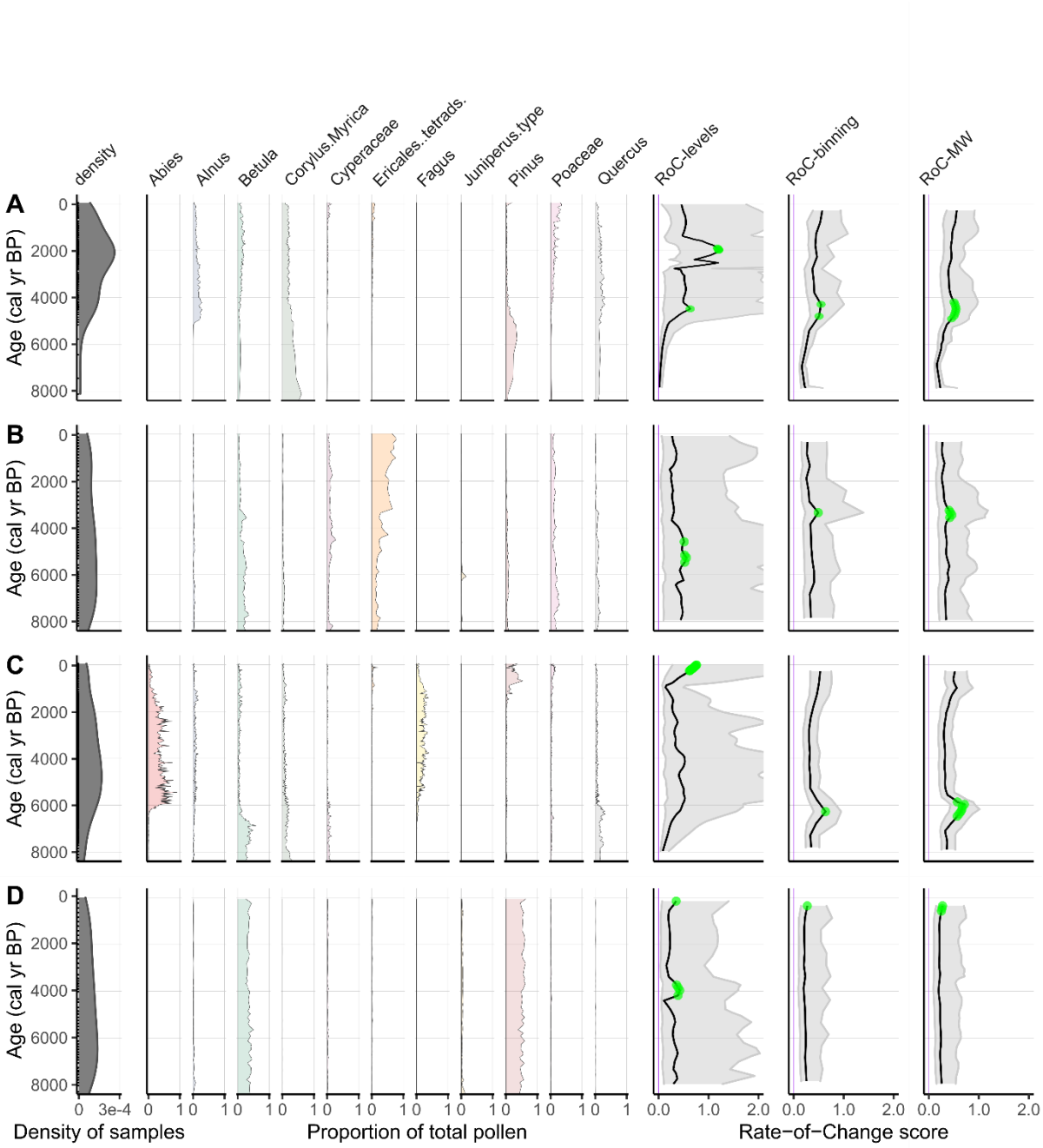

561

562 **Figure 2. Summary of four sequences used in this study**: Glendalough (A), Dallican Water (B),
563 Steerenmoos (C), and Alanen Laanijärvi (D). For each sequence, three different plots are shown.
564 First plot (left) shows the density of levels within each sequence for the last 8000 cal yr. Second
565 plot (middle) shows pollen stratigraphies for the most common taxa in the sequences. Values are
566 presented as proportions of pollen grains in each level. Last plot (right) shows the rate-of-change
567 score calculated with R-Ratepol for three different methods for WU selection: RoC-levels = use of
568 individual levels, RoC-binning = selective binning, RoC-MW = binning with moving window. Age-
569 weighted average and Chi-squared coefficient were selected for smoothing and dissimilarity

570 measure, respectively. Green points indicate significant peak-points detected using the GAM
571 method. For a detailed explanation of the methods, see Supplementary Methods.

572

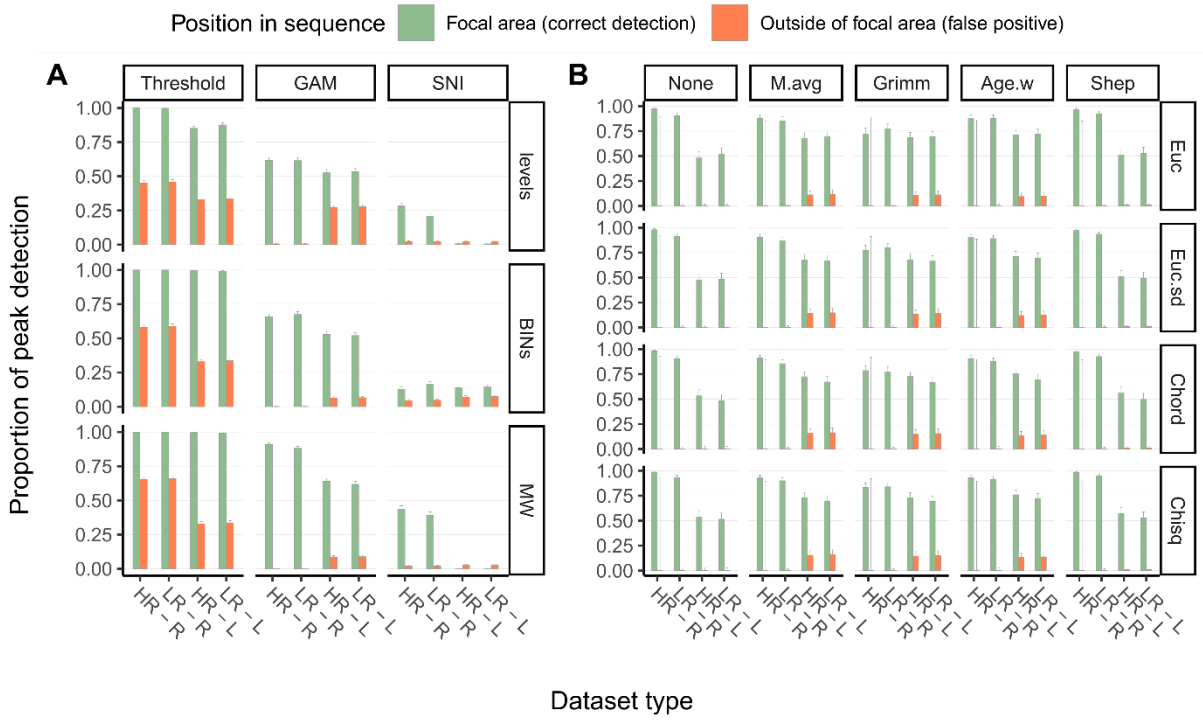

Figure 3. Comparison of the correct detection of peak-points in simulated datasets with a high or low density of levels in datasets of high or low richness. The focal area is the time of the manual edit of the environmental data (Fig. S1). Four types of simulated datasets are used: *low richness – recent manual edit of environmental properties* (LR-R)*, low richness – late position of the change in environmental properties* (LR-L)*, high richness – recent manual edit of environmental properties* (HR-R), and *high richness – late position of the change in environmental properties* (HR-L). A) Comparison of peak-point detection rates between different WU selections and peak-point detection methods. B) Comparison of peak-point detection rates using binning with the moving window and GAM method. Peak-point detection methods: Threshold = Threshold method, GAM = GAM method, SNI = Signal-to-Noise Index method. Working unit selection: levels = use of subsequent levels, BINs = selective binning, MW = binning with moving window. Smoothing methods: None = data without smoothing, M.avg = moving average, Grimm = Grimm's smoothing, Age.w = age-weighted average, Shep = Shepard's 5-term filter. Dissimilarity coefficients: Euc = Euclidian distance, Euc.sd = Standardised Euclidean distance, Chord = Chord distance, Chisq = Chi-squared coefficient. For a detailed explanation of the methods, see Supplementary Methods.

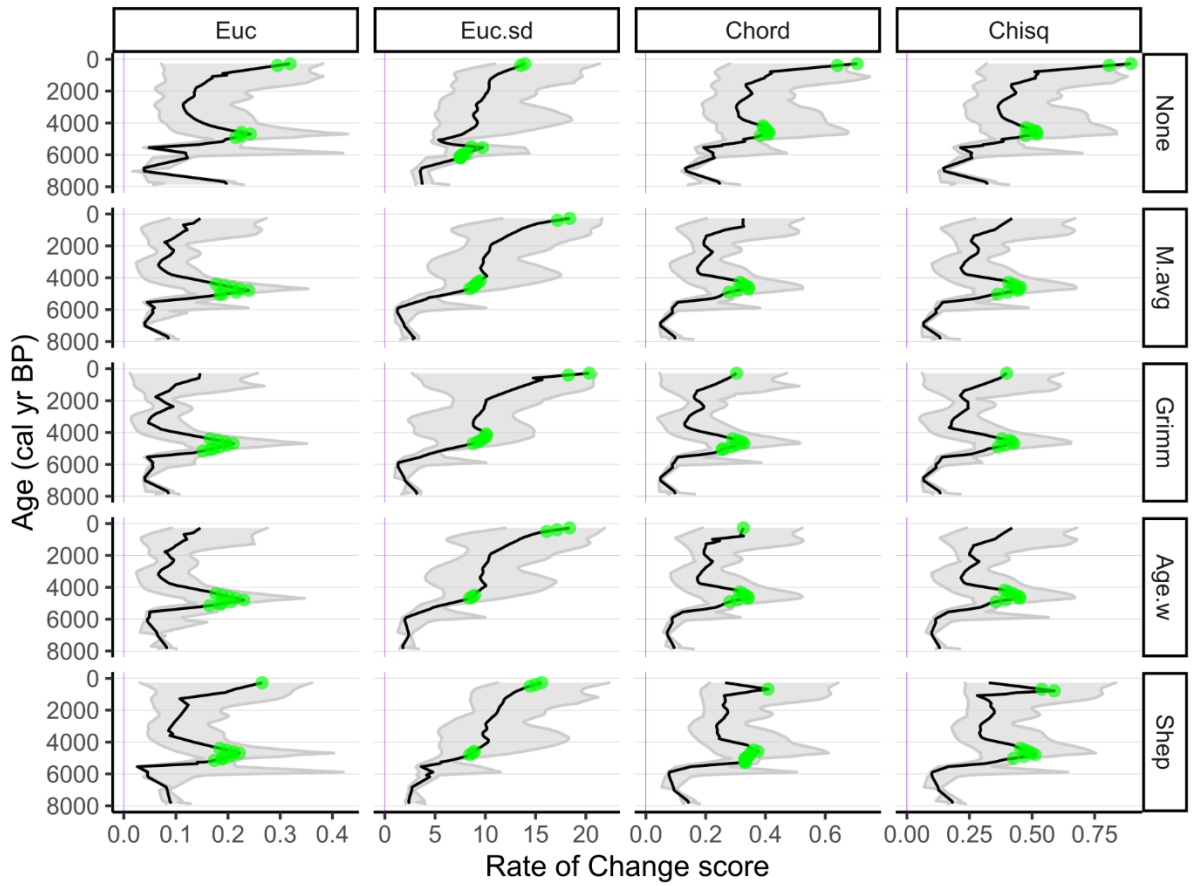

Figure 4. Rate-of-change (RoC) and peak-points detected in Sequence A (Glendalough) for four dissimilarity coefficients (columns) on five categories of data smoothing (rows). Green points indicate significant peak-points detected using the GAM approach. Dissimilarity coefficients: Euc = Euclidian distance, Euc.sd = Standardised Euclidean distance, Chord = Chord distance, Chisq = Chi-squared coefficient. Smoothing methods: None = data without smoothing, M.avg = moving average, Grimm = Grimm's smoothing, Age.w = age-weighted average, Shep = Shepard's 5-term filter. For a detailed explanation of the methods, see Supplementary Methods.